ACS Partner Journal

Journal of the American Society for Mass Spectrometry

pubs.acs.org/jasms

Research Article

Microdroplet Impact-Induced Spray Ionization Mass Spectrometry (MISI MS) for Online Reaction Monitoring and Bacteria Discrimination

Pallab Basuri, Subhashree Das, Shantha Kumar Jenifer, Sourav Kanti Jana, and Thalappil Pradeep*

Cite This: *J. Am. Soc. Mass Spectrom.* 2021, 32, 355−363

Read Online

ACCESS | Metrics & More | Article Recommendations | Supporting Information

ABSTRACT: Microdroplet impact-induced spray ionization (MISI) is demonstrated involving the impact of microdroplets produced from a paper and their impact on another, leading to the ionization of analytes deposited on the latter. This cascaded process is more advantageous in comparison to standard spray ionization as it performs reactions and ionization simultaneously in the absence of high voltage directly applied on the sample. In MISI, we apply direct current (DC) potential only to the terminal paper, used as the primary ion source. Charge transfer due to microdroplet/ion deposition on the flowing analyte solution on the second surface generates secondary charged microdroplets from it carrying the analytes, which ionize and get detected by a mass spectrometer. In this way, up to three cascaded spray sources could be assembled in series. We show the detection of small molecules and proteins in such ionization events. MISI provides a method to understand chemical reactions by droplet impact. The C−C bond formation reactions catalyzed by palladium and alkali metal ion encapsulation using crown ether were studied as our model reactions. To demonstrate the application of our ion source in a bioanalytical context, we studied the noninvasive in situ discrimination of bacteria samples under ambient conditions.

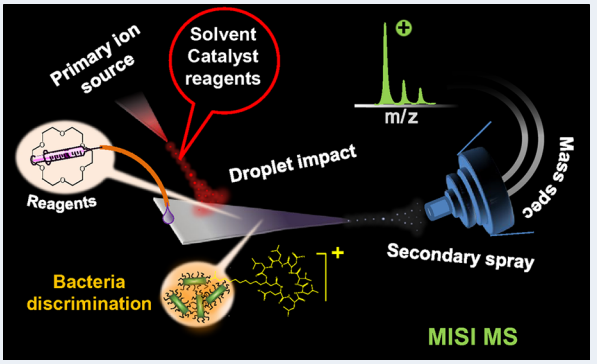

INTRODUCTION

Electrospray ionization and its variations have grown phenomenally in recent years. Paper spray ionization (PSI) is one of them.[1,2] It has provided an easy and direct sampling method in the field of ambient ionization mass spectrometry. In a paper spray technique, a high DC potential is applied to achieve ionization from the tip of a paper in the form of charged microdroplets. However, additional factors such as heat,[3] ultrasonic sound,[4] chemical vapor,[5] solvent,[6] or laser[7] have also been used to assist ionization. Paper spray ionization and its other variants such as leaf spray,[8] spray from a polymer,[9] cloth,[10] cotton thread,[11] and glass[12] have also been used for the analysis of plant metabolites,[13] blood clots,[14] dyes,[15] bio fluids, etc. In all such cases, ion generation is mainly driven by the potential difference between the tip of the substrate and the inlet of the mass spectrometer (MS). Generally, potential on the order of a few kilovolts (kV), which produces a large electric field between the substrate and the inlet of MS, is required to facilitate the ionization process. In-source molecular fragmentation,[16−19] structural or conformational changes,[20] and biological damage of the analyte in large electric field[21,22] are undesired effects of such techniques. These limitations can be due to the generation of large electric field across the electrodes. However, ionization through nanomaterials has helped in reducing a few of the limitations.[23] For example, a carbon nanotube-coated paper reduced the potential required from kilovolts to a few volts.[24] Nano- and microstructural super hydrophobic paper spray[25,26] helped in reaching a very low detection limit. But in comparison to kilovolt paper spray ionization (kVPSI), low voltage ionization is limited by its signal intensity and requires advanced materials for effective ionization.

Another interesting feature of a paper-based device is that a paper due to its inherent fibrous structure can be utilized in microfluidics. The capillarity-driven liquid transport on a paper surface makes it a unique reaction vessel in many cases. Examples include enzymatic reactions, immunoassays, biomarker detection in biomedical applications, detection of heavy metal ions, pesticides, and volatile organic compounds (VOCs) in water for environmental applications and many more.[27] In most of the cases, the detection is performed either by direct colorimetric methods or coupling them with suitable detectors. Distance-based colorimetric detection is another

Received: September 30, 2020
Revised: October 31, 2020
Accepted: November 2, 2020
Published: November 17, 2020

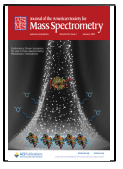

https://dx.doi.org/10.1021/jasms.0c00365
J. Am. Soc. Mass Spectrom. 2021, 32, 355−363

important feature of such paper microfluidics, in which colored product bands get generated during flow along the paper channel due to in situ reaction with predeposited reagents.[28,29] Reactive paper spray MS is being used for online monitoring of reactions on the paper surface, coupled with MS. In this technique, the reagents are being deposited/mixed over the paper surface to react in situ and products are analyzed using an MS, simultaneously. Many organic reactions such as reactions between isothiazolinones and cysteamine,[30] Suzuki-coupling,[31] haloform reaction,[32] quinone derivatization,[33] etc., have been investigated.

Herein, we introduce a new ambient ionization methodology, called microdroplet impact-induced spray ionization mass spectrometry (MISI MS). By this, we established a consecutive ionization process. In MISI, a primary ion source initiates a second paper spray by impinging desolvated ions and/or microdroplets on the latter. MISI provides ionization of analytes without directly applying a high potential to the sample. It supports analysis of live samples in real time. Several analytical methods have been developed for the detection and discrimination of bacteria. Many of them involve complex sample preparation processes such as extraction, purification, and preconcentration requiring expertise on sampling and instrumentation. Enzyme-linked immune assay (ELISA),[34] fluorescence microscopy,[35] polymerase chain reaction (PCR),[36] and biosensors[37] are a few examples of such analyses. However, techniques of this type are often time-consuming where the same sample cannot be measured repeatedly. Mass spectrometry-based detection methods, e.g., matrix-assisted laser desorption ionization (MALDI),[38] pyrolysis gas chromatography (Py GC),[39] electrospray ionization (ESI),[40] desorption electrospray ionization (DESI),[41] and paper spray ionization (PSI),[42] have also been employed in this context. However, most of the techniques are invasive and ineffective for direct live sample analyses.

MISI has been utilized as an online reaction monitoring system which can deliver reagents, catalysts, or solvents through microdroplets. We show that the mechanism of ionization is not due to the applied potential in the primary ion source but due to charge that transfer through interactions of the microdroplets/ions with the molecules on the paper surface during the flow of analyte solution. Many analytes have been ionized through MISI to show the applicability of the method. The technique provides molecular ionization in analytical situations which is often advantageous than standard ionization techniques such as electrospray ionization (ESI), nanoelectrospray ionization (nESI), desorption electrospray ionization (DESI) or kVPSI. We note that the relay mode of ionization (relay electrospray ionization; rESI), which generates secondary electrospray, was first demonstrated by Li et al. where they showed charge deposition onto an array of sample-loaded capillary.[43] They characterized the technique with a few biologically important molecules. Unlike glass capillaries used in rESI, employing a cascaded paper spray mode of ionization in MISI MS provides additional advantages. A few of them are demonstrated in this article and include ionization using immiscible solvents, Pd-catalyzed Suzuki–Miyaura cross-coupling reactions, monitoring ion encapsulation reactions in ambient conditions, controlling reaction dynamics, and discrimination of live bacterial samples in real time.

MATERIALS AND METHODS

Chemicals and sample preparation. The chemicals were bought commercially and were used with no additional processing or purification. *p*-Nitrophenol, glucose, and malic acid were purchased from Avro. Benzothiophene, C_{60}, indole, 18-crown-6, dibenzo-18-crown-6, rhodamine 6G, lysozyme, cytochrome c, and myoglobin were from Sigma-Aldrich. HPLC-grade methanol, toluene, and chloroform were from Sigma or Rankem. Luria–Bertani (LB) broth, nutrient agar, and Mackonkey agar for the culture of bacteria were obtained from HiMedia. *Bacillus subtilis* (ATCC 21331) was a gift from Prof. S. Gummadi (Department of Biotechnology, IITM). *Escherichia coli* (MTCC 443) and *Pseudomonas putida* (MTCC 2467) were obtained from the Microbial Type Culture Collection and Gene Bank. LIVE/DEAD Baclight bacterial viability kit was purchased from Molecular Probes, Eugene, OR.

MISI MS. To build a MISI source, we used a kV PSI technique as the primary ion source, and the charged microdroplets were then impacted to the next paper, as shown in the schematic of Figure 1, to induce a second paper

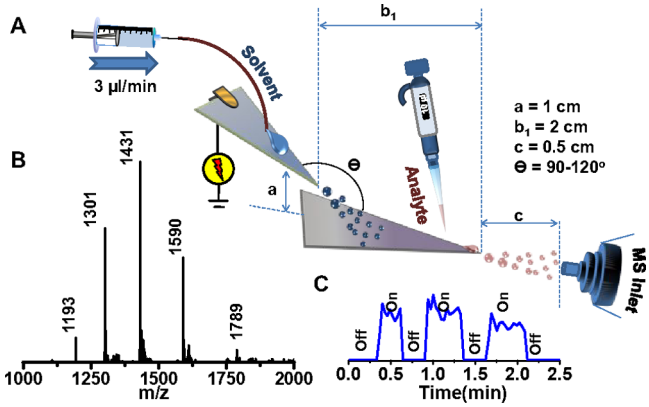

Figure 1. (A) Schematic representation of microdroplet impact-induced spray ionization mass spectrometry (C1), (B) mass spectrum of lysozyme, and (C) chronogram of primary ion source in on/off conditions. The chronogram is for the selected ion at m/z 1431. "On/Off" in the chronogram describes on/off of the primary spray, respectively. *a*, *b*, and *c* represent the distance between the planes of the two paper, tip-to-tip, and tip-to-inlet distance as shown in the schematic of the setup, respectively.

spray ionization. This paper spray couple is termed as cascade 1 (abbreviated as C1). The overall setup is then held in front of a mass spectrometer in such a way that the tip of the second triangular paper is pointed toward the inlet of the spectrometer. The primary ion source can be of any ambient ionization method such as, ESI, nESI or kVPSI, etc. We used kVPSI for our setup. Figure S1 presents the optical image of the setup. In a similar way, cascade 2 (C2) can be fabricated by placing a third paper below the second. This series can continue until the ion generation at the last paper becomes extremely poor. Shape and dimensions of the paper were chosen to be isosceles triangle of 50 mm^2 average area, with 10 mm base length. In the primary paper spray ion source, we ionize solvent molecules such as methanol or water. However, any solvent which can easily generate an electrospray plume is sufficient. Solvents were infused through a fused silica capillary with a preferred flow rate. The flow was driven by a syringe pump. The sample was pipetted on to the second paper and

https://dx.doi.org/10.1021/jasms.0c00365
J. Am. Soc. Mass Spectrom. 2021, 32, 355−363

analyzed immediately while it was still wet. Variable parameters used in MISI MS are the potential used in the primary ion source, the vertical gap between the two papers (termed as "a" taken as 1 cm), the horizontal distance between the two paper tips (termed as "b_i", i = 1, 2, 3) (b_1 = 2 cm, as in Figure 1A), the distance between the tip of the final paper to the MS inlet (termed as "c", set to 1−8 mm), and the angle between the papers (θ, set to 120°), as shown in Figure 1A. The parameters mentioned were used in most experiments and changes, if any, are mentioned.

A Thermo LTQ XL mass spectrometer was used for all the mass spectrometric experiments. Capillary and tube lens voltages were set to ±35 and ±139 V, respectively, to obtain maximum ion intensity for the corresponding positive and negative analysis modes during most of the experiments. The capillary temperature was tuned to 275 °C. The sheath gas flow rate was set to zero.

Online Monitoring of Ion Encapsulation Reactions In-Flow. Chemical reactions involving encapsulation of deposited ions in solution were investigated. We used reagents in the primary ion source instead of solvents alone, and the corresponding dryions or the charged microdroplets containing the solvated ions of the reagent were deposited on other reagent molecules, flowing continuously on the second paper. It is noted that for highly volatile solvents with sufficient flight time these primary microdroplets can desolvate to release and deposit dry ions. In both the cases, the reaction occurs in-flow after the impact of the charged microdroplets/ions in the second paper. Products of the reaction were analyzed in cascade mode using mass spectrometry. To demonstrate such an interaction of the deposited ions with the neutral molecules in-flow, alkali metal ion encapsulation reactions using crown ethers were performed. We used an aqueous solution containing equal concentrations of chlorides of Na, K, Rb, and Cs in the primary ion source. The individual ion concentration of each salt in the mixture was 10 μM. In the second paper, we used 10 μM solutions of two different crown ethers, namely 18-crown-6 and dibenzo-18-crown-6. We drop casted 30 μL of crown ether solution on the paper. The measurement was done in C1 mode. We have also recorded the mass spectrum of the bulk reaction in which the metal salts and the crown ether were mixed in a vial and stored for 30 min before measurement by kVPSI.

The kinetics of a reaction in any microfluidics system is measured by varying the reaction time either by changing the travel distance of the liquid, keeping the flow rate constant or by changing the flow rate for a constant travel distance.[44−46] Ratio of the travel distance and the flow velocity corresponds to the time of mixing or the reaction time. The reaction kinetics is then understood by plotting the relative intensity of the product with time. We have also monitored the kinetics of the alkali metal ion encapsulation in crown ethers using MISI. The experiment was conducted by infusing crown ether continuously on the paper. The mass spectrum was recorded by varying the distance, b_1. The relative intensity ratio of the potassiated and the sodiated peaks were plotted against the distance, b_1. The average terminal velocity of the fluid over the paper surface was also measured by taking the time taken for the liquid front to move a unit distance at a fixed flow rate of 100 μL/min from a syringe pump.

Onsite Delivery of Active Catalyst for C−C Bond Formation in MISI. Palladium-catalyzed C−C, C−O, and C−N bond formation reactions have been of interest to synthetic organic chemistry.[47] Suzuki coupling is one such example where C−C coupling occurs between arylboronic acid and aryl halide in the presence of a catalyst and base.[48] One of the tricky parts of the reaction mechanism is to activate the precatalyst using base for the reaction to proceed further.[49] Research in this area shows different ways to perform such reactions.[50] Online reaction monitoring through mass spectrometry opens new possibilities to understand the chemistry of the catalyst during the reaction. Literature shows that the base eliminates the ligands from the catalyst to activate it. Chen et al. performed a Buchwald coupling reaction using liquid DESI, where the activated catalyst was mixed through channels to the reagent solution before electrospray detection.[51] We utilized MISI as a system to deliver such activated catalyst efficiently to the reagent mixture flowing on a paper surface through droplets. For this we used nESI as our primary ion source which contains the base and the catalyst. The solution was then subjected to spray over the flowing reaction mixture on the paper surface. The flowing reaction mixture contained the base, arylborornic acid, and aryl halide. It should be noted that MISI was used as a preparative tool rather than an analytical method.

We used xphos-Pd-G3 (0.1 mM in ethanol) as our model catalyst. As reagents, we used 4-hydroxyboronic acid, 4-pyridineboronic acid, 6-bromoquinoline, and 4-iodoanisole and saw product formation both in positive and negative modes. Each reagent and base were prepared in ethanol in 1 and 2 mM concentrations. As the microdroplets from the primary spray impacted with the activated catalyst, the reaction was started in-flow and the products finally ended up in the secondary spray and were detected by the mass spectrometer.

In Situ Detection of Bacterial Lipid at Ambient Conditions. Fresh cultures of *B. subtilis*, *E. coli*, and *P. putida* were prepared from their respective stocks by inoculating 0.1 mL in 10 mL of LB broth and culturing at 37 °C, with 210 rpm shaking, to reach late exponential phase. About 100 μL of the culture was drop casted on top of a triangularly cut sterile filter paper. In situ MISI MS was performed by directly placing the bacteria-containing paper in front of the inlet of the mass spectrometer (in C1 mode). Sterile water containing 10% methanol was sprayed on the paper, and it was used along with nutrient solution in the primary ion source. This was then electrosprayed at a potential of 3 kV. The mass spectra in both positive- and negative-ion modes were recorded, each for 1−2 min. The measurements were repeated after 10 min. We have continued this process at least 5 times and checked the viability of the bacteria after the analysis in MISI. In a supportive experiment, *B. subtilis* containing papers were placed on a nutrient agar plate after analysis for replica plating from the filter paper and the colonial growth of viable cells was observed visually.

RESULT AND DISCUSSION

Characterization of the System. One of the major advantages of doing MISI over other spray-based ionization methods is that there is no direct application of high voltage to the analyte. This allows one to bring the paper tip as close as possible (~0.1 mm) to the inlet of the mass spectrometer without causing arc discharge, whereas ESI or PSI requires a minimum distance from the MS inlet to avoid discharge. Lowering the distance resulted in better coupling of the source with the spectrometer. Initial characterization of MISI MS was done with 30 μL of 10 μM aqueous solution of lysozyme. We

https://dx.doi.org/10.1021/jasms.0c00365
J. Am. Soc. Mass Spectrom. 2021, 32, 355−363

used methanol in the primary ion source to generate kVPSI because methanol can be electrosprayed comparatively at a lower kV (1.5−2 kV). We used 2 kV for most of the experiments. The experiment was done in C1 mode. Figure 1B represents the MISI mass spectrum collected using a 3 mm tip to inlet distance (c = 3 mm). The cascade phenomenon was tested by switching on/off the primary ion source. As the primary ion source was switched off, the cascade process got stopped, which inhibits the ionization subsequently. In Figure 1C, we show the spray on/off signal of the chronogram of MISI. A few more protein samples were also analyzed to see the applicability of the setup toward different proteins. Figure S2 presents the MISI mass spectrum of cytochrome c and myoglobin.

We use a similar methodology to show that MISI in C1 mode can ionize a large variety of molecules having different functionalities. We have chosen a few small molecules, such as indole, malic acid, and C_{60}, as shown in Figure 2. In Figure

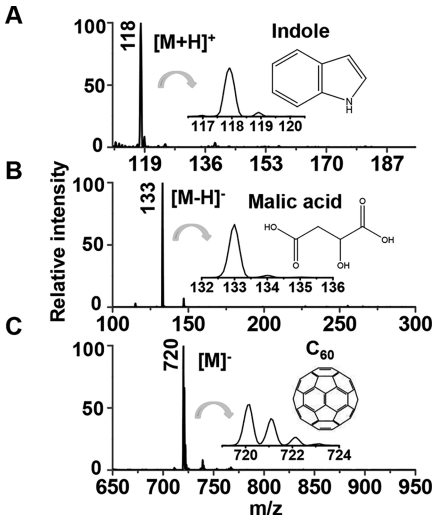

Figure 2. MISI mass spectra of (A) indole, (B) malic acid, and (C) C_{60} in positive- and negative-ion modes. Insets show isotopic distributions of the corresponding mass speaks and the molecular structures of the analytes.

2A,B, we observed the protonated and the deprotonated peaks of indole and malic acid at m/z 118 and 133 in positive- and negative-ion modes, respectively, while a peak at m/z 720 (Figure 2C) is due to the molecular ionization of C_{60} in negative-ion mode. Inset shows the molecular structure and the isotopic distribution of the corresponding analytes. Figure S3 similarly represents MISI MS of nitrophenol, glucose and benzothiophene. Assignments of the mass peaks were made by understanding their MS^2 spectrum. Figure S4 represents the MS/MS spectrum of the corresponding ions of indole, malic acid, and nitrophenol. In an experiment, we demonstrated the cascade behavior of our setup as discussed in Supporting Information 1.

In MISI, ionization occurred through charge transfer from microdroplets to the neutral molecules. The cascade configuration was arranged in such a way (seen in Figure S6) that the microdroplets which are generated at the tip of the first paper impact on the second paper and ionize the analyte present on it. These charged droplets are also formed at the tip of the second paper, which promotes further droplet generation through Coulomb fission at the tip of the same paper, and subsequently, they impact on the next paper in the cascade arrangement. C_{60} in toluene requires 3.5−4 kV to ionize in a standard PSI experiment (Figure 3A). At the same

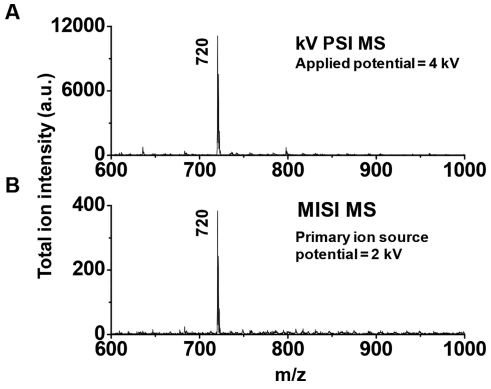

Figure 3. Comparative mass spectra of kVPSI and MISI. (A) kVPSI mass spectrum of C_{60} in toluene (20 μL of 10 μM) at 4 kV in negative-ion mode. (B) MISI mass spectrum of C_{60} in toluene (20 μL of 10 μM) in C1 mode using 2 kV in the primary ion source in which methanol was taken as the solvent. We observed ∼30-fold difference in intensity between the two techniques.

time, MISI required only 1.5−2 kV to generate the electrospray plume in the primary ion source which subsequently ionized C_{60} as shown in Figure 3B. It is noted that any solvent in the primary ion source is suitable to deposit the charge to the second paper. It has also been noticed that the intensity of the C_{60} peak in MISI is 1 order of magnitude less in comparison to kVPSI. To understand the reason behind it, we measured ion current upon droplet impact at each paper in the cascade arrangement. We found that the current due to the secondary spray was less than the primary spray (Figure S9), measured by a picoammeter, connected as shown in the inset of the Figure. This clearly tells that a fraction of charge generated by the primary ion source gets transferred into the liquid, flowing on the subsequent paper due to the charged microdroplets/ions impact. Such charge loss is expected under ambient conditions. The ionization of the analytes flowing on subsequent papers in MISI is then caused by charge transfer occurring on the paper surface by the impact of charged microdroplets/ions with the solution. Loss of charge during deposition also explains the reduction in ion intensity in cascade, as shown previously.

The detection limit of the setup in C1 mode turned out to be 10 nM, measured using R6G in methanol. Figure S10 shows the calibration curve.

MISI MS Monitoring of Suzuki−Miyaura Cross-Coupling Reactions. The catalytic cycle of Suzuki reaction (Figure 4A) shows that NaOEt participates in reductive elimination of carbazole from the xphos-Pd-G3 precatalyst, resulting in the activation of the catalyst. In this step, the success of the Suzuki reaction relies on the rapid delivery of the activated catalyst to the reaction mixture. The activation of the catalyst was done in the primary ion source as shown by the shaded area in Figure 4A. Finally, droplet impact and transport of matter through the fibers of the paper help the reaction to progress. We performed two different reactions as shown in the insets of Figure 4B,D. In the absence of the catalyst in the primary ion source, we observed a peak corresponding to deprotonated 4-hydroxyphenylboronic acid (Figure 4B) at m/z 137 in the negative-ion mode for the first reaction. Similarly,

https://dx.doi.org/10.1021/jasms.0c00365
J. Am. Soc. Mass Spectrom. 2021, 32, 355−363

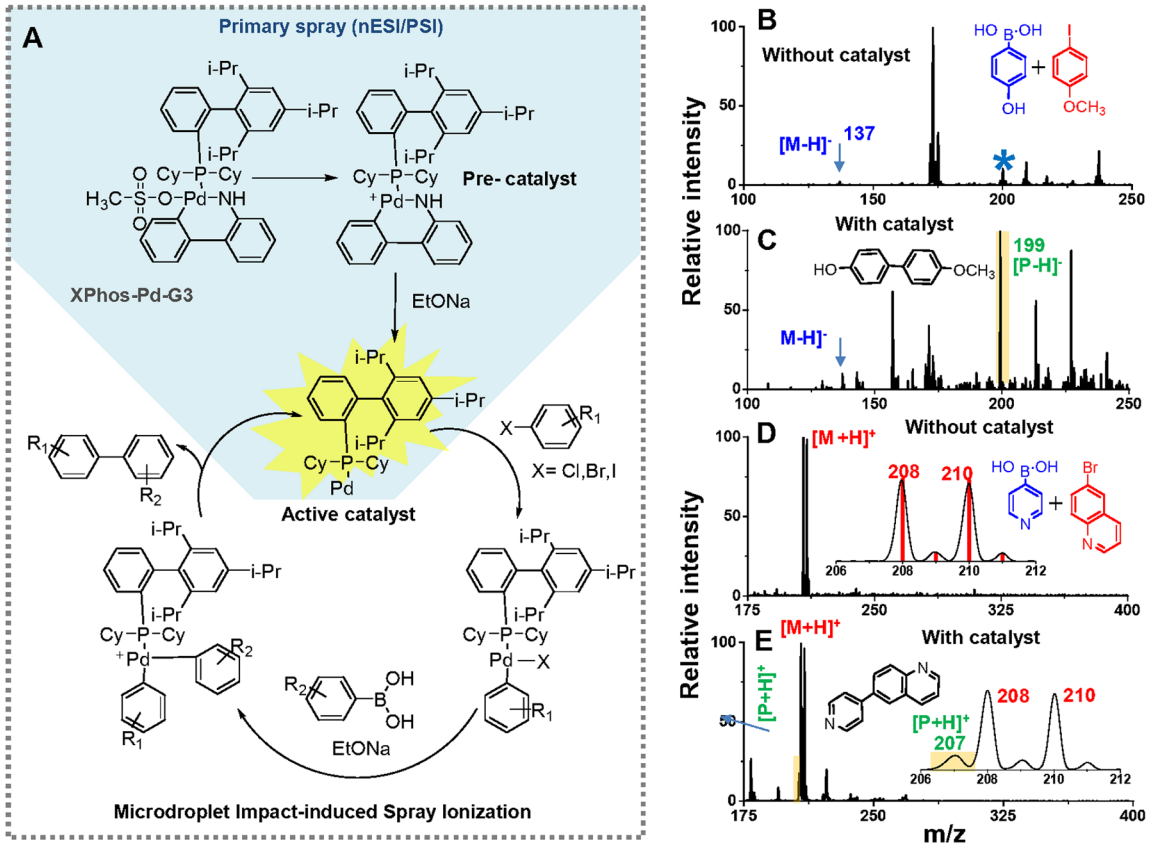

Figure 4. Microdroplet delivery of activated catalyst for online monitoring of Suzuki cross-coupling reaction by MISI MS. (A) Scheme of the catalytic cycle of the reaction using xphos-Pd-G3 catalyst. The sky blue shaded area represents the activation of the catalyst in the primary ion source. The primary ion source can either be nESI or PSI. (B, C) Mass spectra during the reaction between 4-hydroxyboronic acid and 4-iodoanisole in negative-ion mode in the absence and presence of the catalyst. (D, E) Mass spectra for the reaction between 4-pyridinboronic acid and 6-bromoquinoline in positive-ion mode in absence and presence of catalyst. Molecular structure of the reagents and the products are shown at the inset of the respective figure.

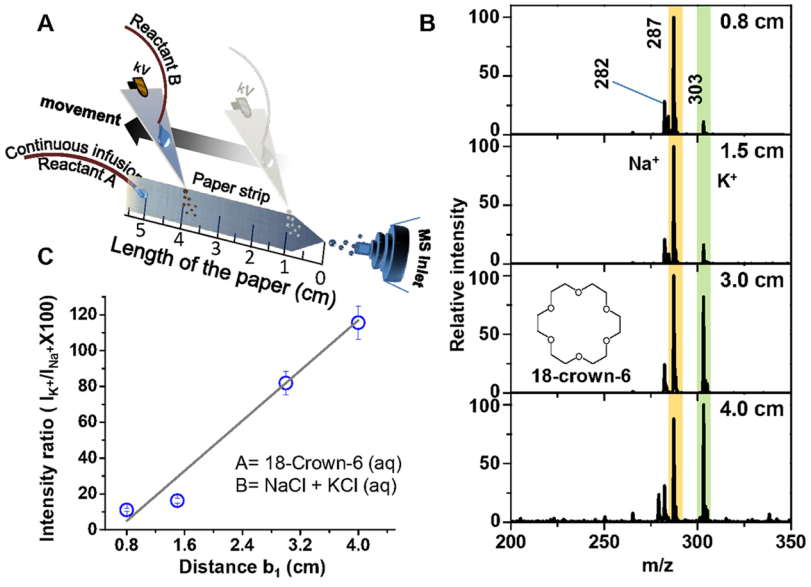

Figure 5. (A) Schematic representation of cascade 1 setup for encapsulation of alkali metal ions in the host, 18-crown-6. (B) MISI mass spectrum of Na^+ and K^+ addition in 18-C-6. Inset: molecular structure of 18-C-6. The yellow shaded area represents the peak for Na^+ added crown ether at m/z 287. Similarly, the green highlighted area shows the signal for the K^+ added crown ether at m/z 303. (C) Intensity ratio of K^+ to Na^+ added peaks vs distance.

https://dx.doi.org/10.1021/jasms.0c00365
J. Am. Soc. Mass Spectrom. 2021, 32, 355−363

the molecular ion peak of 6-bromoquinoline in positive-ion mode at m/z 208 was seen for the second reaction. However, for both the reactions, we observed product peaks when the active catalyst was sprayed. The first reaction between 4-hydroxybrornic acid and 4-iodoanisole gives a deprotonated cross-coupling product at m/z 199 as the base peak (Figure 4C) along with a peak at m/z 137 in negative-ion mode. In the second reaction, between 4-pyridinebroronic acid and 6-bromoquinoline, we observed a protonated product at m/z 207 (Figure 4E) along with a peak at m/z 208 in the positive-ion mode. All the peaks were confirmed by their MSMS data as shown in Figure S11 and S12.

Ion-Encapsulation Reactions. MISI was utilized as a tool to investigate ion encapsulation reactions in situ in solution. This is because in MISI primary charged microdroplets/ions are impacting with molecules that are flowing on another paper surface. To give an example, we have conducted alkali metal ion encapsulation reactions with crown ethers. Figure S13A shows the MISI mass spectrum of the reaction between cations of Na, K, Rb, and Cs with 18-crown-6 in C1 mode. We found a sodiated peak of the crown ether at m/z 287 as the base peak and a peak at m/z 303 for K^+ encapsulation. However, the bulk reaction shows different distribution of the peaks in which addition of all of the metal ions was observed. Figure S13B shows the mass spectrum of the same reaction done in bulk. We found the potassiated peak of the crown ether at m/z 303 as the base peak in addition to the other peaks at m/z 287, 349, and 397 for Na^+, Rb^+, and Cs^+ added crown ether, respectively. Generally, the equilibrium constant of 18-crown ethers for K^+ selection is higher than Na^+ selection for bulk reaction in water.[52] This hints at the fact that the encapsulation products during MISI measurement do not undergo thermodynamic equilibrium. Rather, it may be kinetically controlled. We have also demonstrated a similar phenomenon with another crown ether. The MISI and kVPSI mass spectra using dibenzo-18-crown-6 are presented in Figure S14. In Figure S14A, we see the mass spectrum of the bulk reaction which shows a different distribution than the ion molecule reaction in MISI, as shown in Figure S14B. The scanning electron microscopy images of the triangularly cut paper, in Figure S15, show that the fibers of the paper make a microfluidic system in which liquid transport is driven by capillary force. The reaction might occur during liquid transport through the capillaries of the paper by mixing of the reagents. Hence, if we increase the travel time of the liquid by lengthening the paper, we can increase the reaction time. To do so, we have changed the geometry of the paper. Figure 5A schematically presents such a setup. We have also put a scale on the paper by making pencil marks (which do not interfere with the reaction). Figure S16 shows an optical image of the setup. When we increase the travel distance (or time) by moving the primary spray head toward the base of the labeled paper (or increasing the b value), we see changes in the mass spectrum. For this, we have used equal concentration of sodium and potassium chlorides in the primary ion source. In Figure 5B, we observed that upon increasing b from 0.8 to 4 cm the intensity ratio between the potassiated ($[K(18\text{-C-}6)]^+$ at m/z 303) and the sodiated peaks ($[Na(18\text{-C-}6)]^+$ at m/z 287) increase and finally make a distribution like bulk (Figure S17). A plot of intensity ratio vs distance is shown in Figure 5C, which essentially suggests that the ion encapsulation reaction dynamics change linearly from kinetically controlled to thermodynamically controlled, as the reaction time was increased. In Supporting Information 2, we present the details of terminal velocity calculation. Images taken during the experiment are also shown in Figure S18. The intensity ratio of potassiated and sodiated peaks of 18-crown-6 with respect to the calculated travel time shows similar change in the reaction dynamics with increasing time (Figure S19).

In Situ Monitoring of Live Bacterial Lipid. Having established that molecules over the paper surface experience negligible amount of potential in MISI, we tried to see the compatibility of the setup toward the analysis of live biological samples. For this, we have chosen three different bacterial samples. These were Gram-positive *B. subtilis*, Gram-negative *E. coli*, and *P. putida*.

A high electric field has a lethal effect on bacteria due to the rupture of cell membranes.[22,53,54] PSI is known to produce a large electric field (~10^8 V/cm) between the fibers of the paper as the gap between the fibers are in the micrometer range.[55] Such high electric fields can cause cell death. But MISI provides a noninvasive methodology to discriminate bacteria based on their lipid distribution as there is no high voltage applied directly on the sample. The signal intensity was quite similar to other ambient ionization processes such as electrospray or PSI, as discussed earlier. Figure 6A schematically illustrates the process of analysis in C1 mode using a bacterial sample deposited on a paper. Figure 6B presents the MISI mass spectrum collected in negative-ion mode using *B. subtilis*. The inset shows the lipids in a selected mass range, in which a peak at m/z 1035 is identified as the signature deprotonated peak of surfactin (C15) for this species. This was confirmed using the MS/MS spectrum as shown in Figure S20. Figure 7 shows the lipidomic discrimination of three different bacteria in positive-ion mode. The paper after analysis was kept on saline water medium for controlled growth of bacteria. The entire measurement took place in 1−2 min. The paper was then measured again after 10 min, and similar signals were achieved. This suggests the noninvasiveness of the analysis. The same procedure was repeated at least five times.

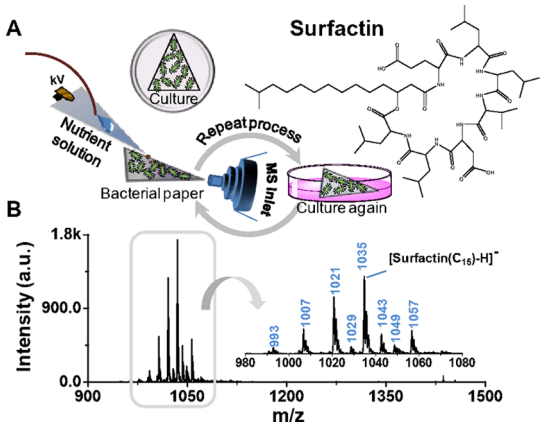

Figure 6. Noninvasive detection of bacterial lipid. (A) Schematic diagram of the experiment. Inset of the figure also shows the molecular structure of surfactin. (B) MISI mass spectrum of the bacterial lipid in negative-ion mode. *B. subtilis* was cultured over a triangularly cut filter paper. Inset shows the zoomed in view of the selected mass range. Deprotonated surfactin (C15) peak is at m/z 1035. The other lipid peaks are indicated on the blue trace which are homologues of surfactin (C15).

Additionally, there were no tedious sample preparation steps involved in this technique. We found that the bacterial cells

https://dx.doi.org/10.1021/jasms.0c00365
J. Am. Soc. Mass Spectrom. 2021, 32, 355−363

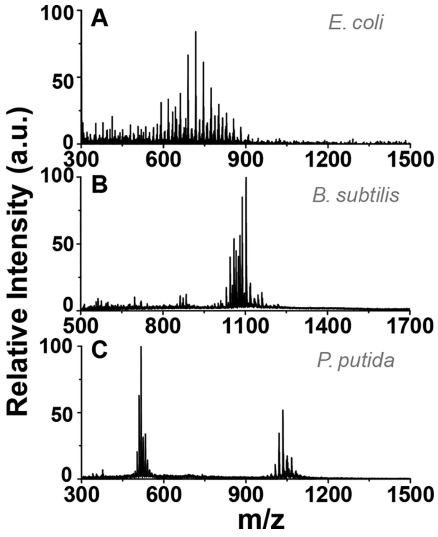

Figure 7. Discrimination of bacteria based on their lipid distribution in the positive-ion mode. MISI mass spectra of (A) *E. coli*, (B) *B. subtilis*, and (C) *P. putida*.

had a viability of 98% after the first analysis. The bacterial cells which were analyzed five times under MISI showed 89% viability, as shown in Figure S21. However, there is a significant reduction in the bacterial count after a single kVPSI experiment according to the replica plating experiment. Similarly, *B. subtilis* cells were also observed to grow on agar plates after they were transferred from the filter paper onto agar plates by placing the paper on the freshly prepared agar plates after analysis (Figure S22). We ensured that the bacteria subjected to MISI were studied for viability.

CONCLUSION

We introduce the method of microdroplet impact-induced spray ionization mass spectrometry (MISI MS), which is more advantageous in comparison to standard kVPSI in terms of absence of high voltage directly applied on the sample. We show that the ionization is due to charge transfer by impact of charged microdroplets on flowing solutions. We have demonstrated three different modes of MISI, termed as C1, C2, and C3. The detection limit of the setup in C1 mode turned out to be 10 nM, measured using R6G in methanol. MISI paved a new way to perform reactions online. The Suzuki coupling reaction is shown as a model example, where the catalyst activation was performed, and the activated catalyst was delivered on the reactant. In this way, many reactions can be performed and monitored online, where the primary spray can be used as a source of catalyst/reagents either by synthesizing them or by delivering them using microdroplets. We have also shown that MISI can help in the noninvasive in situ detection of live bacterial samples. We have discriminated three bacterial species based on their lipid profiles. We have shown that the ionization causes no harm to the bacteria even after five analysis cycles. This indicates that our system can detect metabolites in live samples without electrical field-induced biological changes. Such unique aspects make MISI a novel ambient ionization method to investigate chemical and/or biological transformations in future.

ASSOCIATED CONTENT

Supporting Information

The Supporting Information is available free of charge at https://pubs.acs.org/doi/10.1021/jasms.0c00365.

Experimental data including optical images of the technique, SEM image of the normal paper, MS^n data of the analytes, and mass spectra of other bacterial samples (PDF)

AUTHOR INFORMATION

Corresponding Author

Thalappil Pradeep − *DST Unit of Nanoscience (DST UNS) and Thematic Unit of Excellence (TUE), Department of Chemistry, Indian Institute of Technology Madras, Chennai 600036, India;* orcid.org/0000-0003-3174-534X; Phone: +91-44-22574208; Email: pradeep@iitm.ac.in; Fax: +91-44-2257 0509/0545

Authors

Pallab Basuri − *DST Unit of Nanoscience (DST UNS) and Thematic Unit of Excellence (TUE), Department of Chemistry, Indian Institute of Technology Madras, Chennai 600036, India*

Subhashree Das − *DST Unit of Nanoscience (DST UNS) and Thematic Unit of Excellence (TUE), Department of Chemistry, Indian Institute of Technology Madras, Chennai 600036, India*

Shantha Kumar Jenifer − *DST Unit of Nanoscience (DST UNS) and Thematic Unit of Excellence (TUE), Department of Chemistry, Indian Institute of Technology Madras, Chennai 600036, India*

Sourav Kanti Jana − *DST Unit of Nanoscience (DST UNS) and Thematic Unit of Excellence (TUE), Department of Chemistry, Indian Institute of Technology Madras, Chennai 600036, India;* orcid.org/0000-0001-5772-7022

Complete contact information is available at: https://pubs.acs.org/10.1021/jasms.0c00365

Notes

The authors declare no competing financial interest.

ACKNOWLEDGMENTS

We thank the Department of Science and Technology, Government of India, for equipment support through the Nano Mission. P.B. acknowledges IIT Madras for providing an Institute Doctoral Fellowship.

REFERENCES

(1) Wang, H.; Liu, J.; Cooks, R. G.; Ouyang, Z. Paper Spray for Direct Analysis of Complex Mixtures Using Mass Spectrometry. *Angew. Chem., Int. Ed.* **2010**, *49* (5), 877−880.

(2) Liu, J.; Wang, H.; Manicke, N. E.; Lin, J.-M.; Cooks, R. G.; Ouyang, Z. Development, Characterization, and Application of Paper Spray Ionization. *Anal. Chem.* **2010**, *82* (6), 2463−2471.

(3) Huang, H.; Wu, Q.; Zeng, L.; Wan, L.; Lai, S.; Yin, X.; Huang, J.; Yang, B.; Liu, J. Heating paper spray mass spectrometry for enhanced detection of propranolol in dried blood samples. *Anal. Methods* **2017**, *9* (29), 4282−4287.

(4) Banks, J. F.; Shen, S.; Whitehouse, C. M.; Fenn, J. B. Ultrasonically assisted electrospray ionization for LC/MS determination of nucleosides from a transfer RNA digest. *Anal. Chem.* **1994**, *66* (3), 406−414.

(5) Li, Z.; Li, L. Chemical-Vapor-Assisted Electrospray Ionization for Increasing Analyte Signals in Electrospray Ionization Mass Spectrometry. *Anal. Chem.* **2014**, *86* (1), 331−335.
(6) Zhang, J.-T.; Wang, H.-Y.; Zhu, W.; Cai, T.-T.; Guo, Y.-L. Solvent-Assisted Electrospray Ionization for Direct Analysis of Various Compounds (Complex) from Low/Nonpolar Solvents and Eluents. *Anal. Chem.* **2014**, *86* (18), 8937−8942.
(7) Basuri, P.; Sarkar, D.; Paramasivam, G.; Pradeep, T. Detection of Hydrocarbons by Laser Assisted Paper Spray Ionization Mass Spectrometry (LAPSI MS). *Anal. Chem.* **2018**, *90* (7), 4663−4668.
(8) Liu, J.; Wang, H.; Cooks, R. G.; Ouyang, Z. Leaf Spray: Direct Chemical Analysis of Plant Material and Living Plants by Mass Spectrometry. *Anal. Chem.* **2011**, *83* (20), 7608−7613.
(9) Song, X.; Chen, H.; Zare, R. N. Conductive Polymer Spray Ionization Mass Spectrometry for Biofluid Analysis. *Anal. Chem.* **2018**, *90* (21), 12878−12885.
(10) Silva, L. C. d.; Pereira, I.; Carvalho, T. C. d.; Allochio Filho, J. F.; Romão, W.; Gontijo Vaz, B. Paper spray ionization and portable mass spectrometers: a review. *Anal. Methods* **2019**, *11* (8), 999−1013.
(11) Jackson, S.; Swiner, D. J.; Capone, P. C.; Badu-Tawiah, A. K. Thread spray mass spectrometry for direct analysis of capsaicinoids in pepper products. *Anal. Chim. Acta* **2018**, *1023*, 81−88.
(12) Jiang, J.; Zhang, H.; Li, M.; Dulay, M. T.; Ingram, A. J.; Li, N.; You, H.; Zare, R. N. Droplet Spray Ionization from a Glass Microscope Slide: Real-Time Monitoring of Ethylene Polymerization. *Anal. Chem.* **2015**, *87* (16), 8057−8062.
(13) Freund, D. M.; Sammons, K. A.; Makunga, N. P.; Cohen, J. D.; Hegeman, A. D. Leaf spray mass spectrometry: a rapid ambient ionization technique to directly assess metabolites from plant tissues. *J. Visualized Exp.* **2018**, No. 136, No. e57949.
(14) Bills, B. J.; Manicke, N. E. Development of a prototype blood fractionation cartridge for plasma analysis by paper spray mass spectrometry. *Clinical Mass Spectrometry* **2016**, *2*, 18−24.
(15) Guo, T.; Zhang, Z.; Yannell, K. E.; Dong, Y.; Cooks, R. G. Paper spray ionization mass spectrometry for rapid quantification of illegal beverage dyes. *Anal. Methods* **2017**, *9* (44), 6273−6279.
(16) Gu, J.; Hiraga, T.; Wada, Y. Electrospray ionization mass spectrometry of pyridylaminated oligosaccharide derivatives: Sensitivity and in-source fragmentation. *Biol. Mass Spectrom.* **1994**, *23* (4), 212−217.
(17) Xue, J.; Domingo-Almenara, X.; Guijas, C.; Palermo, A.; Rinschen, M. M.; Isbell, J.; Benton, H. P.; Siuzdak, G. Enhanced in-Source Fragmentation Annotation Enables Novel Data Independent Acquisition and Autonomous METLIN Molecular Identification. *Anal. Chem.* **2020**, *92* (8), 6051−6059.
(18) Gathungu, R. M.; Larrea, P.; Sniatynski, M. J.; Marur, V. R.; Bowden, J. A.; Koelmel, J. P.; Starke-Reed, P.; Hubbard, V. S.; Kristal, B. S. Optimization of Electrospray Ionization Source Parameters for Lipidomics To Reduce Misannotation of In-Source Fragments as Precursor Ions. *Anal. Chem.* **2018**, *90* (22), 13523−13532.
(19) Xu, Y. F.; Lu, W.; Rabinowitz, J. D. Avoiding misannotation of in-source fragmentation products as cellular metabolites in liquid chromatography-mass spectrometry-based metabolomics. *Anal. Chem.* **2015**, *87* (4), 2273−81.
(20) Kostyukevich, Y.; Kononikhin, A.; Popov, I.; Nikolaev, E. Conformational changes of ubiquitin during electrospray ionization as determined by in-ESI source H/D exchange combined with high-resolution MS and ECD fragmentation. *J. Mass Spectrom.* **2014**, *49* (10), 989−994.
(21) Li, D.; Jia, S.; Zhang, L.; Wang, Z.; Pan, J.; Zhu, B.; Luo, Y. Effect of using a high voltage electrostatic field on microbial communities, degradation of adenosine triphosphate, and water loss when thawing lightly-salted, frozen common carp (Cyprinus carpio). *J. Food Eng.* **2017**, *212*, 226−233.
(22) Zimmermann, U.; Pilwat, G.; Riemann, F. Dielectric breakdown of cell membranes. *Biophys. J.* **1974**, *14* (11), 881−899.
(23) Narayanan, R.; Basuri, P.; Jana, S. K.; Mahendranath, A.; Bose, S.; Pradeep, T. In situ monitoring of electrochemical reactions through CNT-assisted paper cell mass spectrometry. *Analyst* **2019**, *144*, 5404.
(24) Narayanan, R.; Sarkar, D.; Cooks, R. G.; Pradeep, T. Molecular Ionization from Carbon Nanotube Paper. *Angew. Chem.* **2014**, *126* (23), 6046−6050.
(25) Damon, D. E.; Davis, K. M.; Moreira, C. R.; Capone, P.; Cruttenden, R.; Badu-Tawiah, A. K. Direct Biofluid Analysis Using Hydrophobic Paper Spray Mass Spectrometry. *Anal. Chem.* **2016**, *88* (3), 1878−1884.
(26) Basuri, P.; Baidya, A.; Pradeep, T. Sub-Parts-per-Trillion Level Detection of Analytes by Superhydrophobic Preconcentration Paper Spray Ionization Mass Spectrometry (SHPPSI MS). *Anal. Chem.* **2019**, *91* (11), 7118−7124.
(27) Yang, Y.; Noviana, E.; Nguyen, M. P.; Geiss, B. J.; Dandy, D. S.; Henry, C. S. Paper-Based Microfluidic Devices: Emerging Themes and Applications. *Anal. Chem.* **2017**, *89* (1), 71−91.
(28) Cate, D. M.; Noblitt, S. D.; Volckens, J.; Henry, C. S. Multiplexed paper analytical device for quantification of metals using distance-based detection. *Lab Chip* **2015**, *15* (13), 2808−2818.
(29) Cate, D. M.; Dungchai, W.; Cunningham, J. C.; Volckens, J.; Henry, C. S. Simple, distance-based measurement for paper analytical devices. *Lab Chip* **2013**, *13* (12), 2397−2404.
(30) Choi, S.; Cha, S. Investigation of Reactions Between Isothiazolinones and Cysteamine by Reactive Paper Spray Ionization Mass Spectrometry (Reactive PSI MS). *Bulletin of the Korean Chemical Society* **2020**, *41* (1), 48−53.
(31) Banerjee, S.; Basheer, C.; Zare, R. N. A Study of Heterogeneous Catalysis by Nanoparticle-Embedded Paper-Spray Ionization Mass Spectrometry. *Angew. Chem., Int. Ed.* **2016**, *55* (41), 12807−12811.
(32) Bain, R. M.; Pulliam, C. J.; Raab, S. A.; Cooks, R. G. Chemical Synthesis Accelerated by Paper Spray: The Haloform Reaction. *J. Chem. Educ.* **2016**, *93* (2), 340−344.
(33) Zhou, X.; Pei, J.; Huang, G. Reactive paper spray mass spectrometry for in situ identification of quinones. *Rapid Commun. Mass Spectrom.* **2015**, *29* (1), 100−106.
(34) Boccatto, E.; Santos, S. A. d.; Mazieri, N. A. O.; Andrade, D. R. d.; Carrazza, F. R.; Yanaguita, R. M. Evaluation of a Rapid Screening Assay for Bacterial Identification (DOT-ELISA) in Fecal Samples from Children. *Rev. Inst. Med. Trop. Sao Paulo* **1997**, *39*, 21−28.
(35) Krause, M.; Rösch, P.; Radt, B.; Popp, J. Localizing and Identifying Living Bacteria in an Abiotic Environment by a Combination of Raman and Fluorescence Microscopy. *Anal. Chem.* **2008**, *80* (22), 8568−8575.
(36) Athamanolap, P.; Hsieh, K.; Chen, L.; Yang, S.; Wang, T.-H. Integrated Bacterial Identification and Antimicrobial Susceptibility Testing Using PCR and High-Resolution Melt. *Anal. Chem.* **2017**, *89* (21), 11529−11536.
(37) Ahmed, A.; Rushworth, J. V.; Hirst, N. A.; Millner, P. A. Biosensors for Whole-Cell Bacterial Detection. *Clin. Microbiol. Rev.* **2014**, *27* (3), 631.
(38) Yang, Y.; Lin, Y.; Qiao, L. Direct MALDI-TOF MS Identification of Bacterial Mixtures. *Anal. Chem.* **2018**, *90* (17), 10400−10408.
(39) Snyder, A. P.; Dworzanski, J. P.; Tripathi, A.; Maswadeh, W. M.; Wick, C. H. Correlation of Mass Spectrometry Identified Bacterial Biomarkers from a Fielded Pyrolysis-Gas Chromatography-Ion Mobility Spectrometry Biodetector with the Microbiological Gram Stain Classification Scheme. *Anal. Chem.* **2004**, *76* (21), 6492−6499.
(40) Hsu, C.-C.; ElNaggar, M. S.; Peng, Y.; Fang, J.; Sanchez, L. M.; Mascuch, S. J.; Møller, K. A.; Alazzeh, E. K.; Pikula, J.; Quinn, R. A.; Zeng, Y.; Wolfe, B. E.; Dutton, R. J.; Gerwick, L.; Zhang, L.; Liu, X.; Månsson, M.; Dorrestein, P. C. Real-Time Metabolomics on Living Microorganisms Using Ambient Electrospray Ionization Flow-Probe. *Anal. Chem.* **2013**, *85* (15), 7014−7018.
(41) Meetani, M. A.; Shin, Y.-S.; Zhang, S.; Mayer, R.; Basile, F. Desorption electrospray ionization mass spectrometry of intact bacteria. *J. Mass Spectrom.* **2007**, *42* (9), 1186−1193.
(42) Hamid, A. M.; Jarmusch, A. K.; Pirro, V.; Pincus, D. H.; Clay, B. G.; Gervasi, G.; Cooks, R. G. Rapid Discrimination of Bacteria by

Paper Spray Mass Spectrometry. *Anal. Chem.* **2014**, *86* (15), 7500−7507.
(43) Li, A.; Hollerbach, A.; Luo, Q.; Cooks, R. G. On-Demand Ambient Ionization of Picoliter Samples Using Charge Pulses. *Angew. Chem., Int. Ed.* **2015**, *54* (23), 6893−6895.
(44) Bringer, M. R.; Gerdts, C. J.; Song, H.; Tice, J. D.; Ismagilov, R. F. Microfluidic systems for chemical kinetics that rely on chaotic mixing in droplets. *Philos. Trans. R. Soc., A* **2004**, *362* (1818), 1087−1104.
(45) Haven, J. J.; Zaquen, N.; Rubens, M.; Junkers, T. The Kinetics of n-Butyl Acrylate Radical Polymerization Revealed in a Single Experiment by Real Time On-line Mass Spectrometry Monitoring. *Macromol. React. Eng.* **2017**, *11* (4), 1700016.
(46) Shastry, M. C. R.; Luck, S. D.; Roder, H. A Continuous-Flow Capillary Mixing Method to Monitor Reactions on the Microsecond Time Scale. *Biophys. J.* **1998**, *74* (5), 2714−2721.
(47) Beccalli, E. M.; Broggini, G.; Martinelli, M.; Sottocornola, S. C-C, C-O, C-N Bond Formation on sp2 Carbon by Pd(II)-Catalyzed Reactions Involving Oxidant Agents. *Chem. Rev.* **2007**, *107* (11), 5318−5365.
(48) Miyaura, N.; Yamada, K.; Suzuki, A. A new stereospecific cross-coupling by the palladium-catalyzed reaction of 1-alkenylboranes with 1-alkenyl or 1-alkynyl halides. *Tetrahedron Lett.* **1979**, *20* (36), 3437−3440.
(49) Melvin, P. R.; Balcells, D.; Hazari, N.; Nova, A. Understanding Precatalyst Activation in Cross-Coupling Reactions: Alcohol Facilitated Reduction from Pd(II) to Pd(0) in Precatalysts of the Type (η3-allyl)Pd(L)(Cl) and (η3-indenyl)Pd(L)(Cl). *ACS Catal.* **2015**, *5* (9), 5596−5606.
(50) Fedick, P. W.; Iyer, K.; Wei, Z.; Avramova, L.; Capek, G. O.; Cooks, R. G. Screening of the Suzuki Cross-Coupling Reaction Using Desorption Electrospray Ionization in High-Throughput and in Leidenfrost Droplet Experiments. *J. Am. Soc. Mass Spectrom.* **2019**, *30* (10), 2144−2151.
(51) Zheng, Q.; Liu, Y.; Chen, Q.; Hu, M.; Helmy, R.; Sherer, E. C.; Welch, C. J.; Chen, H. Capture of Reactive Monophosphine-Ligated Palladium(0) Intermediates by Mass Spectrometry. *J. Am. Chem. Soc.* **2015**, *137* (44), 14035−14038.
(52) Inokuchi, Y.; Ebata, T.; Ikeda, T.; Haino, T.; Kimura, T.; Guo, H.; Furutani, Y. New insights into metal ion-crown ether complexes revealed by SEIRA spectroscopy. *New J. Chem.* **2015**, *39* (11), 8673−8680.
(53) Sale, A. J. H.; Hamilton, W. A. Effects of high electric fields on microorganisms: I. Killing of bacteria and yeasts. *Biochim. Biophys. Acta, Gen. Subj.* **1967**, *148* (3), 781−788.
(54) Pillet, F.; Formosa-Dague, C.; Baaziz, H.; Dague, E.; Rols, M.-P. Cell wall as a target for bacteria inactivation by pulsed electric fields. *Sci. Rep.* **2016**, *6* (1), 19778.
(55) Espy, R. D.; Muliadi, A. R.; Ouyang, Z.; Cooks, R. G. Spray mechanism in paper spray ionization. *Int. J. Mass Spectrom.* **2012**, *325*−*327*, 167−171.

https://dx.doi.org/10.1021/jasms.0c00365
J. Am. Soc. Mass Spectrom. 2021, 32, 355−363